SEGMENTATION-FREE APPROACH TO THE CLASSIFICATION OF THE STRAIN OF THE CAROTID PLAQUE FROM ULTRASOUND IMAGES

by

Marina Victoire

A Thesis
Submitted to the
Graduate Faculty
of
George Mason University
in Partial Fulfillment of
The Requirements for the Degree
of
Master of Science
Electrical Engineering

Committee:

_____	Dr. Siddhartha Sikdar, Thesis Director
_____	Dr. Parag Chitnis, Committee Member
_____	Dr. Dimitrios Ioannou, Committee Member
_____	Dr. Jiayang Sun, Department Chair
_____	Dr. Kenneth S. Ball, Dean, Volgenau School of Engineering
Date:_____	Spring Semester 2021 George Mason University Fairfax, VA

Segmentation-free Approach to the Classification of the Strain of the Carotid Plaque from Ultrasound Images

A thesis submitted in partial fulfillment of the requirements for the degree of Master of Science at George Mason University

By

Marina Victoire
Bachelor of Science
George Mason University, 2007

Director: Dr. Siddhartha Sikdar, Professor
Department of Bioengineering

Spring Semester 2021
George Mason University
Fairfax, VA

DEDICATION

Cette thèse est dédiée à mon papa. Je suis désolée de ne pas avoir fini à temps pour pouvoir partager cet accomplissement avec toi.

ACKNOWLEDGEMENTS

I would like to thank Professor Siddhartha Sikdar and Dr. Amir Khan for their patience, guidance and invaluable technical expertise. I would also like to thank my family for their support and Dr Seema Sud for her words of encouragements.

TABLE OF CONTENTS

Page

LIST OF FIGURES

LIST OF TABLES

Table Page

LIST OF EQUATIONS

Equation Page

LIST OF ABBREVIATIONS

Computed Tomography scan ..... CT scan
Interquartile Range..... IQR
Magnetic Resonance Imaging..... MRI

ABSTRACT

SEGMENTATION-FREE APPROACH TO THE CLASSIFICATION OF THE STRAIN OF THE CAROTID PLAQUE FROM ULTRASOUND IMAGES

Marina Victoire, M.S.

George Mason University, 2021

ThesisDirector: Dr. Siddhartha Sikdar

Carotid atherosclerosis is an arterial disease caused by the accumulation of plaque inside the walls of the carotid artery, a major artery that carries oxygen-rich blood from the heart to the brain. The buildup of plaque inside the artery wall leads to narrowing, or stenosis, which could reduce blood flow to the brain. Rupture of atherosclerotic plaque and resulting embolization places the patient at an increased risk of stroke. Determining plaque composition can help determine which patients are at higher risk of having a stroke. High risk plaques have been shown to have a thin fibrous cap and a lipid rich necrotic core [22]. One method to determine the composition of the plaque is to measure the amount of strain, and hence, deformation that the plaque endures during a cardiac cycle. Large deformation of plaque are indicative of softer lipid-rich necrotic tissues whereas minimal deformation tend to indicate harder, mostly calcified or fibrotic tissues.

Under the strain of repeated cardiac cycles (heartbeats), plaques may rupture, and small pieces of fibrofatty emboli or blood clots (thrombi) may separate from the plaque and lodge themselves in smaller arteries in the brain leading to a stroke. Ultrasound imaging is a non-invasive, widely available medical tool that has become an attractive imaging modality for initial evaluation of carotid artery stenosis. In previous research [1], images from ultrasound videos of thirteen patients diagnosed with carotid stenosis were processed to measure the amount of deformation of the plaque from one ultrasound image to the next using an algorithm called 'optical flow'. In each image, the carotid plaque was manually segmented before applying the optical flow. In this thesis, we demonstrate that only the first image of each video needs to be segmented and that fitting a bounding box around the area of interest and propagating that bounding box to the rest of the images produce similar results, which greatly reduces the need for tedious manual segmentation. After applying the optical flow algorithm to the area within the bounding box, a clustering algorithm is applied to classify the patients into two distinct groups: (1) a low-risk group where there is minimal deformation of the plaque tissues (less strain) and, (2) a high-risk group where there is large deformation of the plaque tissues (more strain). These classifications of the elasticity of the carotid plaque provide an invaluable initial step to assess which patients might benefit from further diagnosis to better assess the risk of embolization.

INTRODUCTION

Early, affordable, and less invasive diagnosis of carotid atherosclerosis can help save lives. Carotid atherosclerosis is a disease of the carotid artery caused by the buildup of plaque inside the artery walls (Fig. 1). This disease is responsible for up to 25% of strokes nationwide [23].

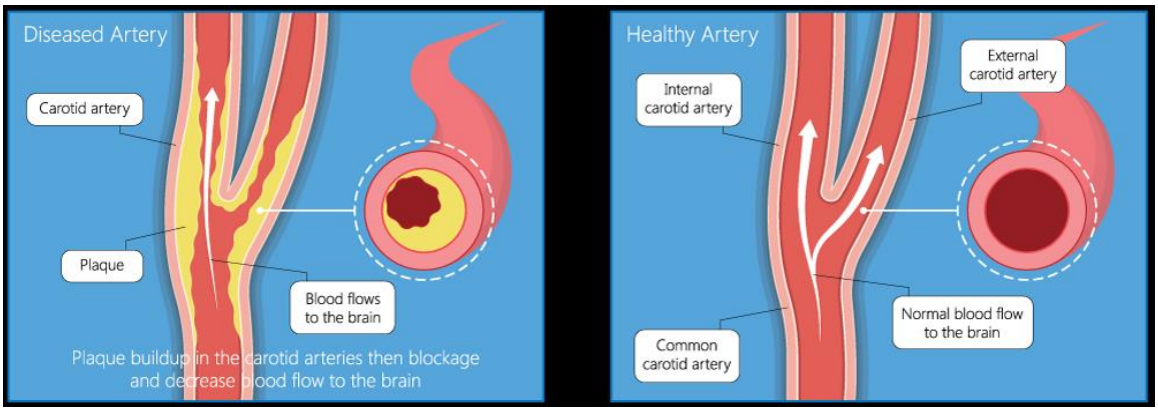

Figure 1 depiction of the carotid plaque [17]

The ability to characterize early the type of plaque a patient has within the carotid artery can be used to determine the patient's risk level for strokes. Plaque composition that is primarily calcium or fibrotic tissues tends to be more rigid, and hence, less likely to detach from the artery wall [9]. Under the strain of repeated cardiac cycles, plaques with a large lipid-necrotic core and a thin fibrous cap are considered to be most likely to

rupture in small pieces of fibrofatty emboli or blood clots (thrombi) and travel up to the brain to lodge themselves in smaller arteries causing a stroke [22]. Currently, the methods of determining the composition of carotid plaques are expensive and invasive, including Magnetic resonance imaging (MRI), computerized tomography (CT) scan, or surgical sampling. Expensive and invasive techniques like these prevent people from getting diagnosed during a routine medical appointment. Diagnosis via ultrasound imaging has become an area of research due to its low cost, less invasive nature, and commonly available medical instrumentation.

In the literature, the main method investigated to assess the deformation of the carotid plaque is to first automatically, or semi-automatically, segment out the plaque in all the images of an ultrasound video. Then, the segmented area is measured to quantify the changes from one ultrasound image to the next. If the measured deformation is large, the patient is classified as having a high risk for stroke. Conversely, if the deformation is minimal, the patient is considered at low risk for stroke.

The selected algorithms that have been investigated as part of this thesis to achieve automatic or semi-automatic segmentation propagation are the following:

Level set method

The level set method is a methodology that was added to the active contour algorithm to mitigate the shortcomings of active contour for image segmentation [10]. If successful, the level set method would clearly identify the contour of the plaque deposit within the

ultrasound image. Generally, the level set method considers the outline of a region of interest as if it was a two dimensional slice of a 3-D surface. That first slice is designated as level set zero. The algorithm then tracks the evolution of that level set to successive level sets of higher values leading to an evolving contour. The level set method evolves the contour/curve by minimizing the energy associated to the current contour as a sum of internal and external energies [5]. The objective function to be optimized is:

Equation 1 Level Set objective function

$$J(c) = \int_c (E_{int}(r(s)) + E_{ext}(r(s))ds$$

where c is the curve, E_{int} is the internal energy, E_{ext} is the external energy and $r(s)$ are the points on the curve.

Figure 2 shows the results on one ultrasound video when I applied the Level Set method. It had trouble detecting the edges of the plaque accurately.

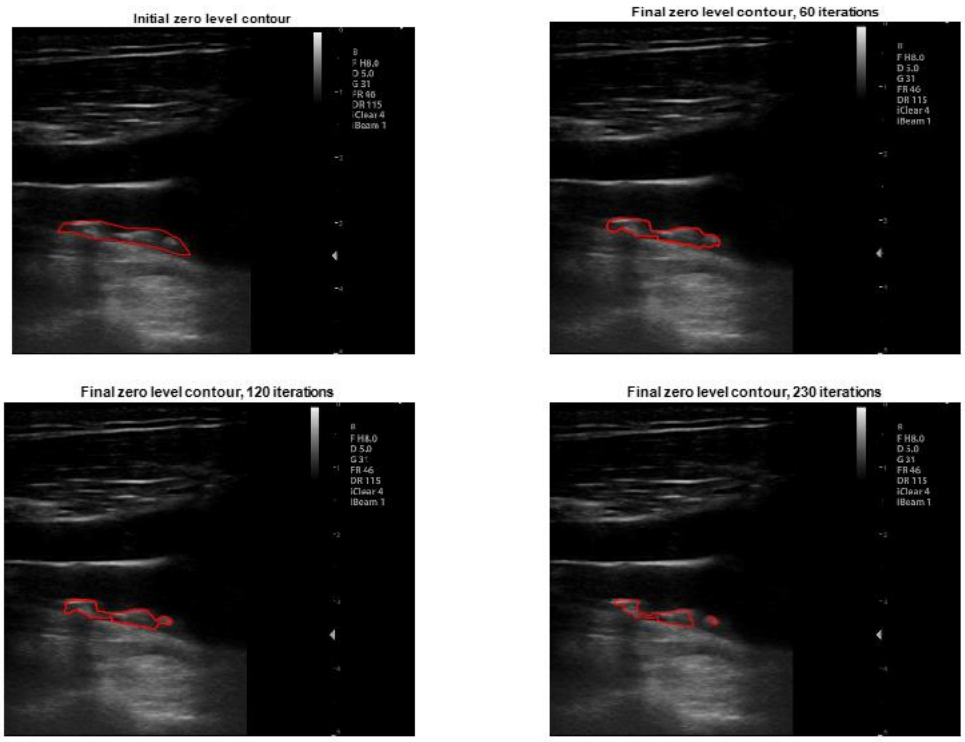

Figure 2 Level set method results on one ultrasound video

Normalized Graph Cuts

Graph cut is an alternative type of edge detection algorithm to level set. Applied to the ultrasound image, successful application of this algorithm would result in identification of the outer edge of the plaque present within the image of the ultrasound. The pixels are like nodes in a weighted graph. This algorithm tries to partition objects within the image by grouping the pixels based on some criterion [3]. This results in higher probability assigned to groups of pixels that are related by this criterion. The partitioning is based on global impressions rather than on local variations. Graph cut uses the criterion to measure

both the total dissimilarity between different groups of pixels as well as the total similarity within the groups of pixels. By optimizing this criterion, the result is an image where the edges of objects are detected. The normalized graph cut normalizes the cut function to minimize bias towards small sets of points.

Equation 2 Normalized Cut

$$Ncut(A,B) = \frac{cut(A,B)}{assoc(A,V)} + \frac{cut(A,B)}{assoc(B,V)}$$

where A and B are two groups of nodes, $A \cup B = V, cut(A,B) = \sum_{u \in A, v \in B} w(u,v)$, $u\ and\ v\ are\ the\ nodes\ and\ w\ the\ weights$

Figure 3 shows the results I obtained while trying the Normalized Cut method on ultrasound images.

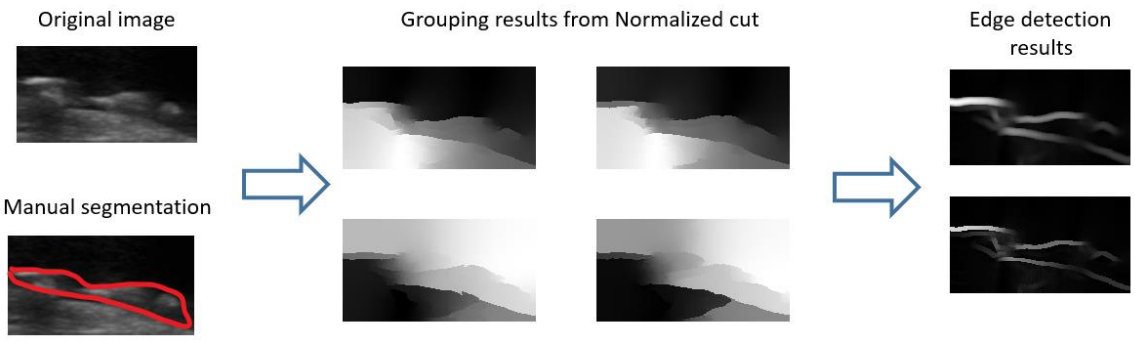

Figure 3 results for one ultrasound image using Normalized cut

Optical flow

Optical flow is an algorithm that estimates the motion of a pixel from two consecutive images. Applied to the ultrasound images, optical flow can provide analysis of apparent plaque deformation between successive images from the ultrasound video. Gibson first proposed this algorithm in 1950 [18]. To approximate the optical flow vectors, a few assumptions are first made which related the brightness patterns in the image to the neighboring pixels. Optical flow is a robust algorithm that is often used in image recognition and computer-generated imagery in games and movies.

Both level set evolution and normalized graph cuts approaches were tested as part of the research for this thesis on ultrasound images of patients with carotid stenosis. Both methods failed at segmenting the plaque in every image. The main reason was that the ultrasound images were too noisy for those algorithms to be successful. The level set method suffered from convergence issues and required re-initialization after a few images. The normalized graph cuts method had difficulties detecting the edges of the plaque when the edges were not clearly distinguishable due to the noisy nature of ultrasound imaging.

Research conducted for this thesis revealed that segmentation of all the images in an ultrasound video may not be necessary to classify the risk level of the different patients. This study demonstrates that applying a bounding box around the plaque and computing the motion of the pixels within that box yields similar results to computing the pixels' motion within the segmented plaque. In other words, the research for this thesis indicates

it is not necessary to segment the plaque from the images to identify the relative deformation of the plaque (confined within an applied bounding box). This is important, since it is the magnitude of the deformation of the plaque over a cardiac cycle that indicates the composition of the plaque, and hence, the risk level of the patient to a stroke.

In this thesis, the optical flow algorithm was selected to measure the strain of the plaque because it proved to be a robust algorithm in contrast to the others discussed previously.

This thesis is organized as follows: First, the method to measure deformation of the plaque is described. Second, this process is applied to data in [1] to obtain experimental results from the clinical data. Third, the experimental results are validated against independent clinical diagnosis. Finally, a summary of the findings and suggested future research is provided.

METHOD

Description of the Optical Flow algorithm

Optical flow is an image processing algorithm. It is used to measure the *apparent* motion of all the pixels in a sequence of images. It has many applications besides the medical field such as video compression, denoising and coding, plant growth analysis, games, image resizing, pedestrian detection and ocean currents studies among others [6,7]. The classical optical flow algorithm which is based on the original formulation of Horn and Schunck [11] makes two main assumptions for a sequence of images:

- Assumption 1 is called the data term: the value of the intensity for a small region persists from one image to the next even if the pixels have moved. This is also referred to as the brightness consistency constraint. Mathematically, this constraint is written as:

Equation 3 Assumption 1 for the data term

$$I(x+u, y+v, t+1) = I(x, y, t)$$

where $I(x, y, t)$ is the image intensity function of a pixel with coordinates x and y at time t (or in image 1), and u and v are the horizontal and vertical displacements (flow velocities) (Fig. 2 and 3). $t + 1$ represents the consecutive image 2 of the pair of images on which the optical flow is computed.

- Assumption 2 is called the spatial term: in real images, regions are often homogeneous; neighboring pixels generally have similar properties (intensity, color, texture, etc.) and therefore belong to the same surface/region. A Markov random field is a probabilistic model that captures this spatial term. If those pixels belong to the same region, it can be assumed that they have a similar motion. This assumption is also known as the spatial smoothness constraint. Below is the mathematical representation of the second assumption:

Equation 4 Assumption 2 for the data term

$$u_p = u_n$$

where $n \in G(p)$, u_p is the horizontal displacement of a pixel and u_n is the horizontal displacement of a neighboring pixel, $G(p)$ is the region/surface of pixels around pixel p. In other words, the spatial derivative of the optical flow field is zero.

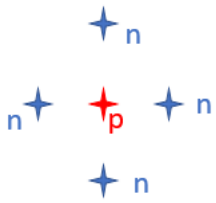

Figure 4 pixel p and neighboring pixels n

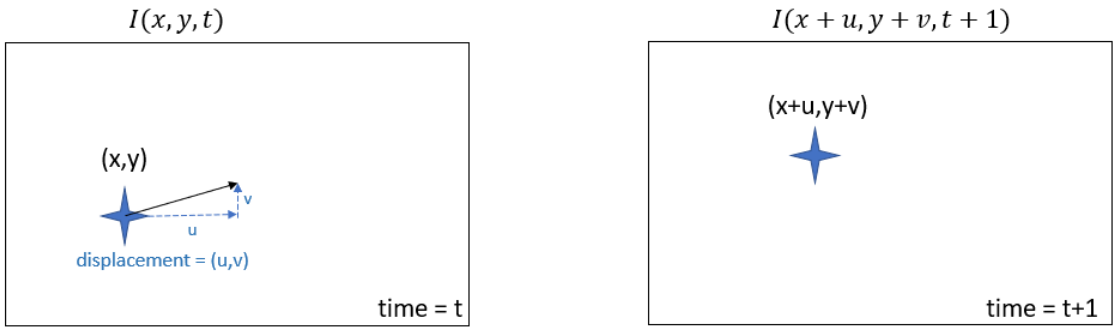

Figure 5 optical flow for a single pixel

Given these two assumptions, an objective function is formulated by combining the data and spatial terms as follows:

Equation 5 Data term

$$E_D(u, v) = \sum_s \big(I(x_s + u_s, y_s + v_s, t + 1) - I(x_s, y_s, t)\big)^2$$

The Data term E_D, a function of the flow vectors, horizontal (u) and vertical (v) components, is the sum of all the pixels in the image and a quadratic penalty function is added. The quadratic error function implies Gaussian noise.

Equation 6 Spatial term

$$E_S(u,v) = \sum_{n\in G(s)}(u_s - u_n)^2 + \sum_{n\in G(s)}(v_s - v_n)^2$$

The spatial term E_S is a function of the flow field and it is a pairwise Markov random field term of all the pixels in the image. The assumptions for the spatial term are that the flow field is smooth, the deviations are Gaussian, and the flow derivative is approximated by first differences.

An energy function combines the two terms:

Equation 7 Energy function

$E(u,v) = E_D(u,v) + \lambda E_S(u,v)$ where λ is a weighting term.

This energy function is the classical formulation of the optical flow objective function.

To compute the flow vectors of each pixel in an image, one needs to solve the objective function (optimization problem) for the flow vectors u and v in equation 5.

The original formulation of Horn and Schunck [11] has sub-optimal assumptions and additional issues such as over-smoothing and sensitivity to outliers. Much research has been published to mitigate those issues. D. Sun and S. Roth found that by applying a median filter to intermediate flow values during incremental estimation and warping, the

results are significantly improved, and the algorithm robustly reject outliers. The details of the enhanced optical flow algorithm from D. Sun and S. Roth can be found in [6].

Processing flow of the method

The method proposed in this research can only be applied on ultrasound videos where at least one image in each video has the carotid plaque segmented. Figure 6 describes the main steps involved in the method.

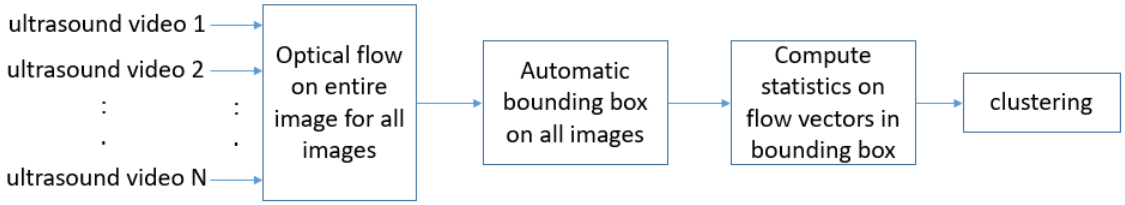

Figure 6 overall block diagram of the bounding box method

For each ultrasound video, the following steps are applied:

- The enhanced optical flow algorithm is applied to each sequential pair of images, outputting the motion vector of each pixel (Fig. 9). Each flow vector has a horizontal component ($\vec{u}$) and a vertical component ($\vec{v}$).
- Automatic creation of a bounding box ten pixels away from the edges of the segmented plaque in the first image of the video. It is considered very unlikely

that the plaque would deform greater than ten pixels from the edge; therefore, ten pixels is a conservative number to use for this application (Fig. 5). From the optical flow 'images', only the vectors within the bounding box are kept for further analysis.

- Median value and IQR (Interquartile Range) of $\vec{u}$ are computed for each optical flow map.

Then, the maximum values of the median value and IQR of $\vec{u}$ for each video are collected. Using those metrics, a clustering algorithm is applied to create two separate, non-overlapping groups. Each grouping represents either a large or small plaque deformation derived from high or low $\vec{u}$.

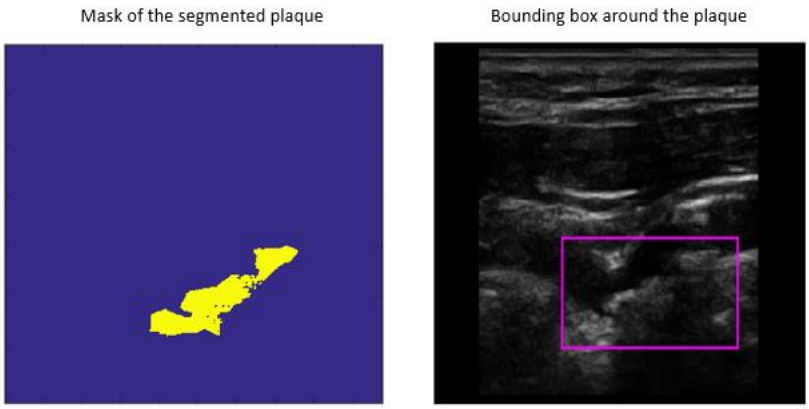

Figure 7 (left) manually segmented plaque, (right) automatic bounding box few pixels away from the edges of the segmented plaque

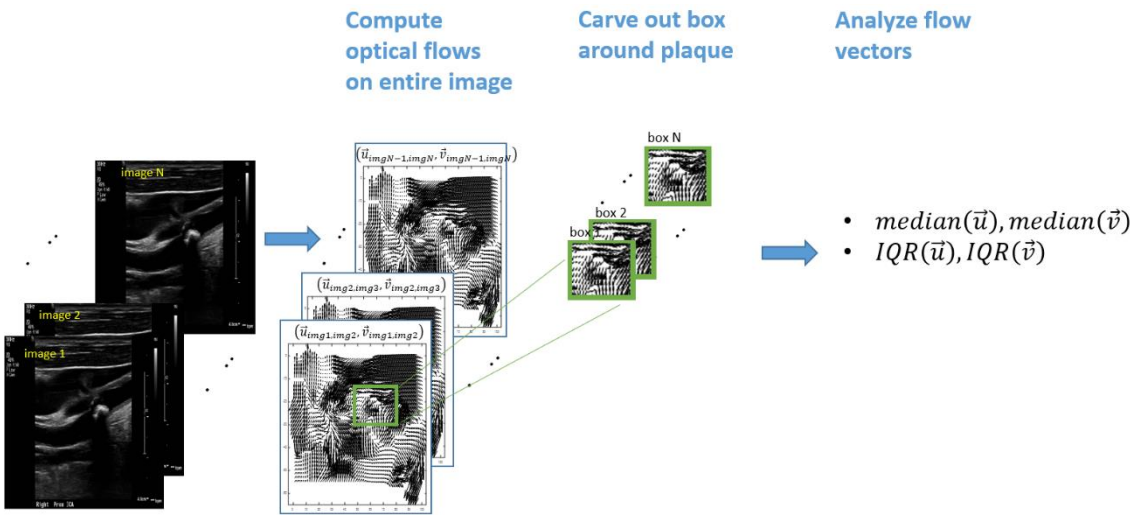

Figure 8 optical flow analysis per ultrasound video/patient

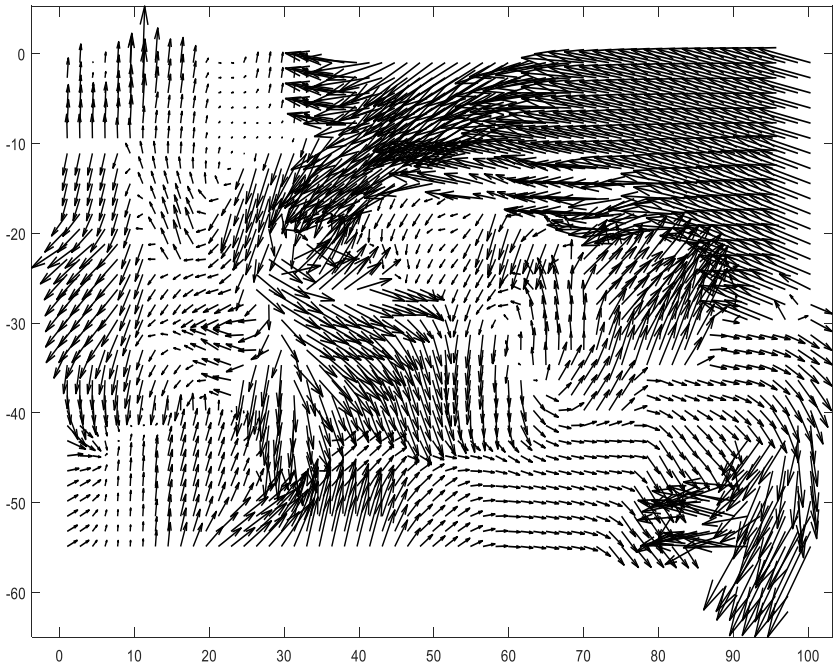

Figure 9 vector flows map for a pair of sequential images

EXPERIMENTAL RESULTS

Experiment set up

For this study, the experiment consisted of comparing the bounding box accuracy with the accuracy of segmenting the plaque in all images. The process steps above (applied to the bounding box) were repeated with the flow vectors within the segmented plaque. In other words, the process above was separately applied twice, once to the flow vectors within the segmented box, and again to the flow vectors within the segmented plaque boundary, for comparison purposes (Fig. 8).

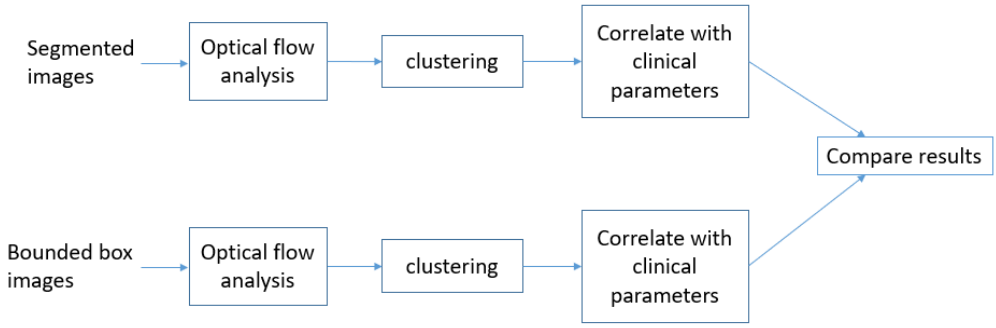

Figure 10 comparison flow diagram of bounding box method and segmentation method.

The clinical data set used for this experiment consists of thirteen ultrasound B-mode cine-loops from thirteen different patients diagnosed with carotid stenosis with a mean age of 70 years old. More than half of those patients exhibited no symptoms during routine

clinical scanning. The number of ultrasound images varies for each patient from 26 to 61 images and each video includes at least one cardiac cycle. In the data set, all images had the carotid plaque outlined by a medical technician.

In figure 11, the median and IQR of $\vec{u}$ and $\vec{v}$ for one patient's ultrasound video are plotted. A couple of observations can be noted about those plots:

- The spikes in the IQR plots correspond to the heartbeat of the patient, which confirms that the optical flow algorithm does capture the motion of the carotid plaque. It is expected that the greatest deformation of the plaque occurs at heartbeat intervals.
- Figure 11 also shows the statistics of the motion vectors for both the bounding box and the segmentation approach show close agreement (overlap), further indicating that application of a bounding box may be a suitable alternative to segmentation of all the images.

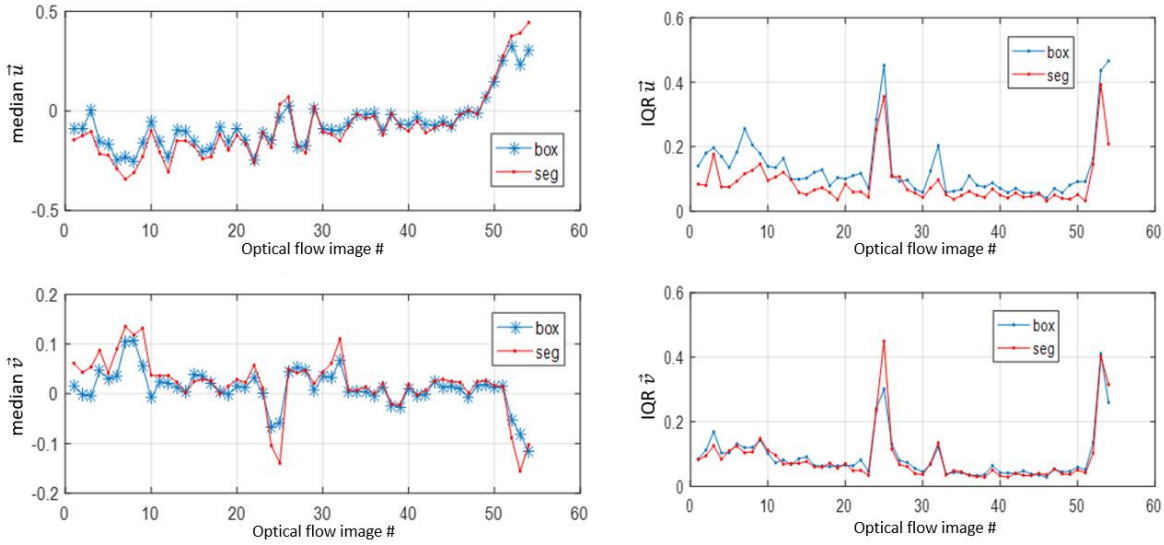

Figure 11 median and IQR of the horizontal displacement u and vertical displacement v of the flow vectors for one ultrasound video. Both bounding box and segmentation approaches are displayed on the same plots.

To separate the high-risk from low-risk patients, some metrics (markers) of the deformation of the plaque need to be defined.

For this application, the statistics of the horizontal displacement $\vec{u}$ were more informative than those of the vertical displacement $\vec{v}$, indicating that most of the deformation occurs in the $\vec{u}$ direction. Therefore, only the statistics of $\vec{u}$ were used as metrics of the deformation of the plaque.

The Interquartile Range (IQR) computes the difference between the first and third quartiles of a data set. IQR captures the variability of the data better than the standard deviation when the data set has outliers. A large IQR means that there is a great amount

of strain on the plaque. For each patient's ultrasound video, the following metrics are computed:

- Metric 1 for Pat_xx = $max\left(max(\vec{u} - median(\vec{u}))_{img(1\rightarrow N)}\right)$, the median is subtracted for normalization.
- Metric 2 for Pat_xx = $max\big(\, max(IQR(\,\vec{u}\,))_{img(1\rightarrow N)}\big)$.

To compare the classification results with the ones in [1], the same clustering algorithm (k-means) is applied to the statistics of the flow vectors for the bounding box approach. K-means clustering is one of the simplest machine learning classification algorithms. K-means performs iterative calculations that attempt to group together data points that are closest to each other, i.e. create separate "clusters" of similar data points related by certain characteristics. The letter k in k-means represents the number of non-overlapping clusters one wishes to obtain, a user-defined target. Figure 12 plots the metric 1 vs metric 2, that is, k-mean clustering results for both the bounding box data set and the segmented data set.

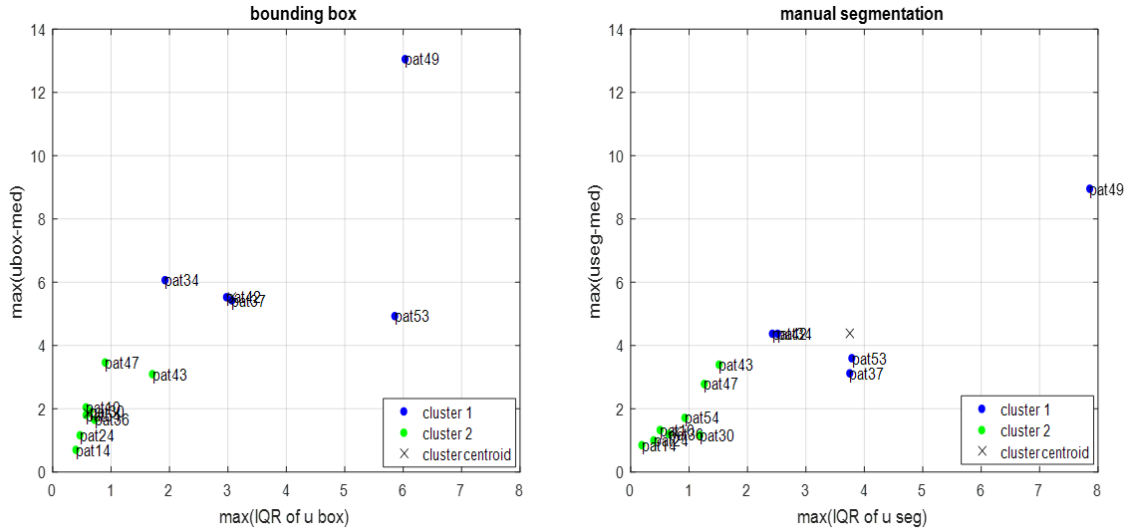

Figure 12 comparison of clustering for bounding box (left) and segmented (right) for the same data set

In figure 12, the clusters are the same whether the plaque is segmented or outlined by a bounding box (Table 1). Table 1 represents further support to the observation made in Figure 12 that both the bounding box and segmentation approaches lead to similar results. Specifically, Table 1 shows the k-means clustering algorithm gave identical cluster results for both the bounding box and segmentation approaches.

The cluster furthest away from the origin of the plot (cluster 1) represents the patients whose carotid plaque exhibit the most deformation, therefore; this cluster is predicted to represent the highest-risk patients. The cluster of predicted low-risk patients is closest to the origin (cluster 2), representing minimal deformation as observed in their ultrasound.

Table 1 Comparison of clustering for bounding box data set (left) and segmented data set (right). The patients highlighted in green belong to the high-risk group

bounding box	segmented
pat10	pat10
pat14	pat14
pat24	pat24
pat30	pat30
pat34	pat34
pat36	pat36
pat37	pat37
pat42	pat42
pat43	pat43
pat47	pat47
pat49	pat49
pat53	pat53
pat54	pat54

Validation of the experimental results

A Bland-Altman (BA) plot is a method that was proposed in 1983 by J. Martin Bland and Douglas G. Altman to determine whether two techniques have a high correlation, and therefore, are both valid approaches by constructing limits of agreement. These statistical limits are computed by calculating the mean and the standard deviation of the differences between two quantitative measurements. The results are displayed graphically in a scatter plot (xy) with the y-axis representing the difference between the

paired measurements, and the x-axis displaying the mean of the paired measurements (Fig. 13). Bland and Altman recommend that 95% of the data points should lie within $\pm 1.96\sigma$ of the mean difference, a high correlation between the two methods exists. In Figure 13, the majority of the data points are within $\pm 1.96\ \sigma$ of the mean difference μ, which confirms that the bounding box method yields similar results as the segmentation method and is a valid method to measure the deformation of the carotid plaque.

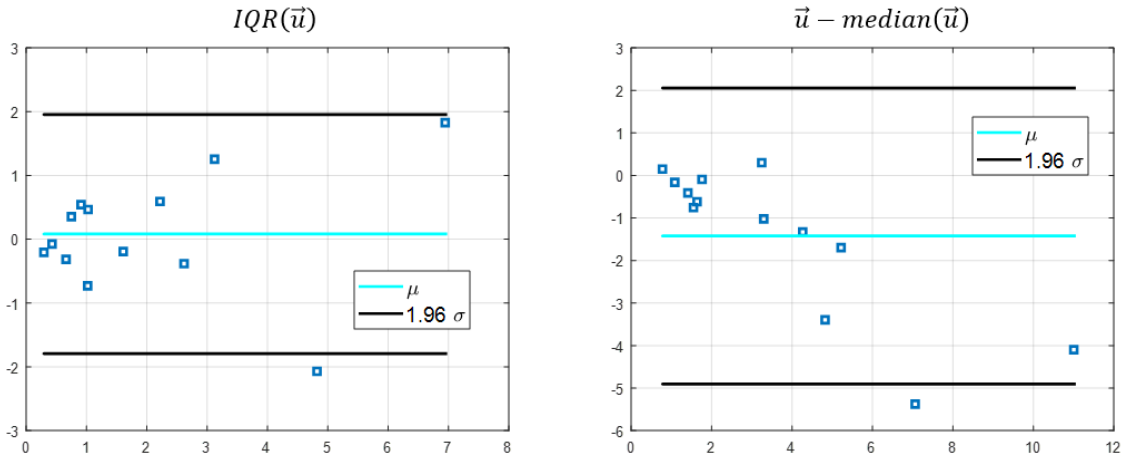

Figure 13 Bland Altman plots to validate measurements from bounding box and segmentation methods.

As a final check on the correlation between this thesis' process of applying the optical flow algorithm to successive ultrasound images, followed by clustering of flow vectors within the bounding box, experimental results presented in this thesis are compared to independent clinical diagnosis as described in [1]. This independent clinical diagnosis

evaluated the same patients used to generate Figures 11, 12, and 13, as well as Table 1. However, the patients' cardiac plaque deformations were independently generated by methods different than those presented in this thesis, and represent an independent clinical diagnosis. The results of those comparisons are presented in Table 2 below.

Table 2 Comparison of clustering for bounding box data set (left) and segmented data set (middle) with independent clinical diagnosis (right). The patients highlighted in green belong to the high-risk group.

bounding box	segmented	Clinical Diagnosis
pat10	pat10	Low Disp.
pat14	pat14	Low Disp.
pat24	pat24	Low Disp.
pat30	pat30	Low Disp
pat34	pat34	High Disp.
pat36	pat36	Low Disp.
pat37	pat37	High Disp.
pat42	pat42	High Disp.
pat43	pat43	Low Disp.
pat47	pat47	Low Disp.
pat49	pat49	High Disp.
pat53	pat53	High Disp
pat54	pat54	Low Disp.

As the results above suggest, the methods of cardiac plaque deformation estimation presented in this thesis have a high correlation to methods used to evaluate a patient by clinical diagnosis. This is especially important given that the methods of clinical

diagnosis may not be pragmatic for routine office visits, but ultrasound equipment and image processing are becoming more common tools used by physicians to diagnose conditions during routine office visits. In addition, the application of the bounding box to the first ultrasound image (in contrast to complete segmentation of the plaque boundary) provides a simpler application of image processing while retaining high confidence in an accurate diagnosis.

Experimental results on another, larger set of clinical data

The bounding box method was applied to a larger set of clinical data (44 patients) where only the first image in each ultrasound video had the carotid plaque outlined by a clinician. This data was then processed using the same methods described earlier for the original 13 patients. Specifically, vector flow was deduced from successive images using the optical flow algorithm and applying a bounding box and clustering of resultant data was performed via a k-means algorithm. The results shown in figure 14, are promising: there is a strong indication that the green cluster corresponds to patients in the high-risk category and the blue cluster would represent the patients in the low-risk category.

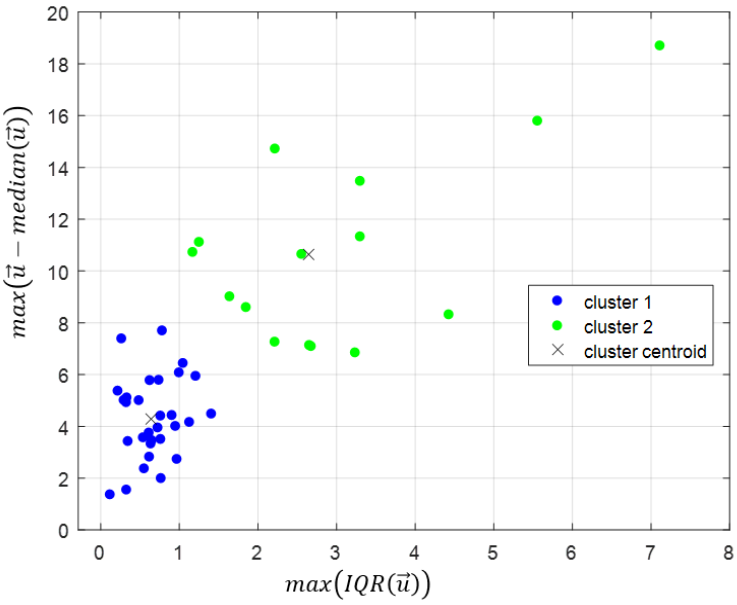

Figure 14 clustering results for 44 patients using the bounding box method.

CONCLUSION

The results presented in this thesis demonstrate the enhanced optical flow algorithm [6] to be a suitable method to measure and quantify the deformation of carotid plaque in ultrasound images. For those patients diagnosed with carotid atherosclerosis , ultrasound imaging has become a non-invasive medical procedure, widely available within the medical community, and can be utilized in routine medical appointments to assess whether a patient requires a more invasive procedure to manage his/her carotid atherosclerosis. In this study, it has been demonstrated that by drawing a simple bounding box a few pixels away from the edges of the segmented plaque in the first image of a patient's ultrasound, and then automatically propagating that box to the remainder of successive images comprising the ultrasound video, one can determine whether that patient is at a higher risk of having a stroke by analysis of the images' vector flow and subsequent clustering of data. The preliminary results presented in this study are promising but should be the first step towards validating this method more rigorously with a greater clinical data set containing labeled data. Future work would benefit from investigation into what size of bounding box maximizes accuracy, or better understand why a more relaxed outline (such as a bounding box) apparently works as well as segmenting out the plaque boundary altogether. This latter aspect may identify specific characteristics of the data within the bounding box relevant to further study. The modified optical flow algorithm from Sun and Roth was optimized for computer

generated images and photography images. Ultrasound imaging uses a different sensor, therefore, looking into optimizing the optical flow algorithm for ultrasound imaging is an area of research worth pursuing.

APPENDIX

Definition of terms

- MRI: Magnetic Resonance Imaging.
- CT scan: Computerized Tomography scan. It produces a more detailed image of the organs, bones, and other tissues of the human body than a regular X-ray device. In a CT scan machine, a narrow X-ray beam circles around the body creating a series of images from different angles. A computer then processes those images to create an image of the cross section of the body.
- B-mode ultrasound cine-loop: Brightness-mode ultrasound. It is a 2-D ultrasound image display composed of bright pixels generated by the ultrasound echoes.
- Embolization: medical procedure to remove blockage in the carotid artery due to the accumulation of plaque.
- IQR: Interquartile range. It is the distance between the 1^{st} and 3^{rd} quartile marks of a set of numbers.

REFERENCES

[1] Khan, A., Sikdar, S. et al. (2017) *Non-invasive characterization of Carotid Plaque Strain.* J Vasc Surg.

[2] Zamani, M. et al. (2020). *Advanced ultrasound methods in assessment of carotid plaque instability: a prospective multimodal study*. BMC Neurology.

[3] Shi, J. and Malik, J. *Normalized Cuts and Image Segmentation*.

[4] Luo, L., Liu, S. et al. (2019) *Carotid artery segmentation using level set method with double adaptive threshold (DATLS) on TOF-MRA images*. Magnetic Resonance Imaging.

[5] Li, C., Xu, C. (2010) *Distance Regularized Level Set Evolution and Its Application to Image Segmentation.* IEEE transactions on image processing, Vol. 19.

[6] Sun, D., Roth, S., Black, M. (2010) *Secrets of Optical Flow Estimation and Their Principles*.

[7] Sun, D., Roth, S., Black, M. (2014) *A Quantitative Analysis of Current Practices in Optical Flow Estimation and the Principles Behind Them*. Int J Comput Vis.

[8] Nandalur, K., Hardie, A. et al. (2007) *Composition of the Stable Carotid Plaque.* NIH.

[9] Berman, S., Wang, X. et al. (2015) *The relationship between carotid artery plaque stability and white matter ischemic injury.* NeuroImage: Clinical 9

[10] Jiang, X., Zhang, R. et al. (2012) *Image Segmentation Based on Level Set Method.* Physics Procedia 33.

[11] Horn, B., Schunck, B. (1981) *Determining optical flow.* Artificial Intelligence, 16:185-203.

[12] Zamani, M., Skagen, K. et al. (2020) *Advanced ultrasound methods in assessment of carotid plaque instability: a perspective multimodal study.* BMC Neurology, 20:39

[13] Belmont, B., Park, D. et al. (2017) *An Open-Source Ultrasound Software for Diagnosis of Fistula Maturation.* ASAIO Journal.

[14] Lu, M., Tang, Y. et al. (2015) *A real time displacement estimation algorithm for ultrasound elastography.* Computers in Industry 69.

[15] Canny, F. (1986) *A computational approach to edge detection.* IEEE transactions on Pattern Analysis and Machine Intelligence.

[16] Haidekker, M. (2011) *Survey of fundamental image processing operators.* Advanced Biomedical Image Analysis

[17] **https://altairhealth.com/altair-health-neurovascular-center/carotid-stenosis/**

[18] Gibson, J. (1950) *The Perception of the Visual World.* Houghton Mifflin.

[19] Loizou, C. (2014) *A review of ultrasound common carotid artery image and video segmentation techniques.* Med Biol Eng Comput.

[20] Baroncini, L., Filho, A. et al. (2007) *Histological composition and progression of carotid plaque.* Thrombosis Journal.

[21] Gepner, A., Colangelo, L. et al. (2015) *Carotid Artery Longitudinal Displacement, Cardiovascular Disease and Risk Factors: The Multi-Ethnic Study of Atherosclerosis.*

[22] Saam, T., Hatsukami, T. et al. (2007) *The Vulnerable, or High-Risk, Atherosclerotic Plaque: Noninvasive MR Imaging for Characterization and Assessment.* Radiology, Vol. 24.

[23] Weinberger, J. (2005) *Diagnosis and prevention of atherosclerotic cerebral infraction.* CNS Spectr.

[24] Naghavi, M., Libby, P., et al. (2003*) From vulnerable plaque to vulnerable patient: a call for new definitions and risk assessment strategies—part I.* Circulation 2003;108: 1664 –1672

BIOGRAPHY

Marina Victoire was born in Bordeaux, France. She came to the United States after high school to pursue an electrical engineering degree at George Mason University in 2003. She graduated magna cum laude with a bachelor's degree in electrical engineering in 2007 specializing in digital signal processing and micro-electronics. She was employed at the Lockheed Martin maritime systems and sensors for 4 years after graduating and then joined the Aerospace corporation.